Rationalizing Phase Transitions with Thermal Annealing Temperatures for P3HT:PCBM Organic Photovoltaic Devices

ARTICLE *in* MACROMOLECULES · FEBRUARY 2012

Impact Factor: 5.8 · DOI: 10.1021/ma202063k

7 AUTHORS, INCLUDING:

Tao Wang
Wuhan University of Technology
51 PUBLICATIONS **757** CITATIONS
SEE PROFILE

Paul A. Staniec
Diamond Light Source
24 PUBLICATIONS **658** CITATIONS
SEE PROFILE

Athene Donald
University of Cambridge
328 PUBLICATIONS **9,597** CITATIONS
SEE PROFILE

Macromolecules

Article

pubs.acs.org/Macromolecules

Rationalizing Phase Transitions with Thermal Annealing Temperatures for P3HT:PCBM Organic Photovoltaic Devices

Andrew J. Pearson,* Tao Wang, Richard A. L. Jones, and David G. Lidzey*

Department of Physics and Astronomy, The University of Sheffield, Hicks Building, Hounsfield Road, Sheffield, S3 7RH, U.K.

Paul A. Staniec

Diamond Light Source, Harwell Science & Technology Campus, Didcot Oxfordshire, OX11 0DE, U.K.

Paul E. Hopkinson and Athene M. Donald

Department of Physics, Cavendish Laboratory, University of Cambridge, JJ Thomson Avenue Cambridge, CB3 0HE, U.K.

Supporting Information

ABSTRACT: We have studied a range of organic photovoltaic devices (OPVs) based on a thin-film blend of P3HT and PCBM and show that, by comparing device studies with a characterization of the thermal transitions of the blend, we can provide a mechanistic description of the optimum annealing temperatures necessary to improve the operational efficiency of a device. For as-cast P3HT:PCBM blend thin-films we evidence two glass transition temperatures corresponding to the existence of two compositionally different amorphous states; an observation that is unreported to date. We demonstrate that an improvement in device efficiency only occurs once the film has been heated above the upper apparent glass transition temperature of the blend. If annealing is performed above the optimum temperature, excessive phase-separation and a partial reduction in film optical density leads to a general decrease in device efficiency. Both of these characteristic temperatures are dependent upon the composition of the blend. The temperature-dependent competition between such processes therefore opens a "window" within which device efficiency can be optimized and provides an opportunity to design effective annealing protocols for future polymer:fullerene blend OPVs.

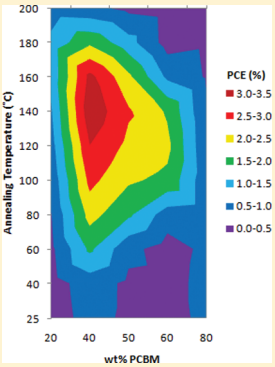

INTRODUCTION

Organic photovoltaics (OPVs) are an emerging technology for renewable energy generation.[1] Such devices can be manufactured at low-cost using processes suitable for large-area deposition.[2] OPVs may also find application in niche applications where, as an example, mechanical flexibility is required.[3] Recent attention has focused on synthesizing new materials[4,5] and designing manufacturing processes[2,6] that lead to the production of efficient and stable devices. To date, the most efficient OPVs have been based on a bulk-heterojunction architecture, with power conversion efficiencies (PCEs) approaching 8% reported for low-bandgap benzodithiophene copolymer: functionalized fullerene blends.[7]

Many groups have explored the fabrication of OPVs based on a blend of the polymer poly(3-hexylthiophene) (P3HT) with the electron acceptor (6,6)-phenyl C61-butyric acid methyl ester (PCBM). While the PCE of this system is limited to between 4 and 5%[8,9] it provides a model system to probe the relations between material structure and device physics in OPVs. In particular, previous studies have focused on the effects of postdeposition treatments on photovoltaic properties.[10−12] These treatments can modify the structure of the films[13,14] permitting processes such as optical-absorption, charge-carrier generation, transport and collection to be optimized.[15] A number of studies have now shown that by thermally annealing a P3HT:PCBM device at a temperature of between 120 and 150 °C for a duration of between 10 and 120 min, device efficiency can be optimized.[8,9,16,17] Variations in material properties and device processing history provide some explanation for the range of reported temperature and time combinations. Nevertheless, a purely empirical approach to device optimization cannot provide a full understanding of this processing step, nor provide a framework in which to design annealing protocols for new blend materials.

We have recently studied the thermal transitions of P3HT:PCBM blend films using dynamic mechanical thermal analysis (DMTA).[18] Our work complements similar studies on the same system performed using different analytical techniques[19,20] with the advantage that the samples used for analysis are prepared in a manner with a greater similarity to OPV devices. In a DMTA experiment, thermal transitions are identified by peaks in a plot of tan δ vs temperature.[18] We

Received: September 9, 2011
Revised: December 9, 2011
Published: January 24, 2012

   dx.doi.org/10.1021/ma202063k | Macromolecules 2012, 45, 1499−1508

monitored the blends during the first heating cycle—thus exploring the properties of the blends during a heating process that is representative of the thermal annealing protocol used to process devices. We showed that the glass transition temperature (T_g) of the P3HT phase within the blend films increased with increasing weight fraction of PCBM (wt %), until the PCBM underwent partial phase separation in the as-cast film. Beyond this threshold concentration (which we measured at 66 wt % PCBM), a relative reduction in the T_g of the P3HT phase suggested a reduced concentration of PCBM mixed within the polymer phase.

In this paper, we apply the findings of our DMTA study to the thermal annealing protocol used to optimize the efficiency of OPVs, and characterize the properties of P3HT:PCBM blend thin-films and OPVs that have undergone a number of annealing conditions. A key technique that we use is spectroscopic ellipsometry (SE) which is used to characterize the thermal transitions of thin-film P3HT:PCBM blends by monitoring their expansion and contraction as they are heated. We confirm that the T_g of P3HT containing phases within the blend thin-films increases as the relative fraction of PCBM in the blend is increased from 20 to 60 wt %. A relative decrease is observed in T_g in a blend thin-film containing a PCBM loading of 80 wt %. We also show that for some blend compositions, two T_g transitions can be detected; an observation that is as yet unreported to date. We find that the higher temperature T_g defines the minimum annealing temperature for an OPV for which an improvement in device efficiency can occur. We show that by annealing a film above this temperature, residual casting solvent is removed, and the film is driven by phase separation between P3HT and PCBM into a nanoscale morphology that is more favorable for efficient device operation. Annealing at temperatures in excess of optimal processing conditions however results in both excessive phase separation of PCBM and a relative blue shift in the optical density of the film, limiting its ability to efficiently harvest light and transport charge. This optimum annealing temperature is dependent on the composition of the thin-film blend and decreases with increasing wt % of PCBM. We are therefore able to understand the origin of the process "window" over which thermal annealing has a beneficial effect on device efficiency. Such understanding will be of clear benefit in designing processing routes for new polymer:fullerene OPV systems.

RESULTS AND DISCUSSION

We first revisit the effects of thermal annealing on the power conversion efficiency (PCE) of a P3HT:PCBM device. Although it has been previously shown that the film composition range yielding the best devices utilizing this blend system is between 40 and 50 wt % PCBM[8,9] it is instructive to probe a broader region of parameter space to give greater insight into the thermal response of the blend thin-films. In Figure 1a, we present the measured PCE of devices having a PCBM content between 40 and 60 wt % as a function of annealing temperature. The PCE of devices containing 20 wt % and 80 wt % PCBM are shown in Figure 1b. Device metrics and external quantum efficiency spectra are provided in the Supporting Information, Figures S1 and S2.

In Figure 1a, we again demonstrate the significant improvements in device efficiency that can result from thermal annealing.[8,21] We find that power conversion efficiencies (PCEs) can be improved from less than 1% for all blend ratios, to up to 3.4% in a device containing a blend composed

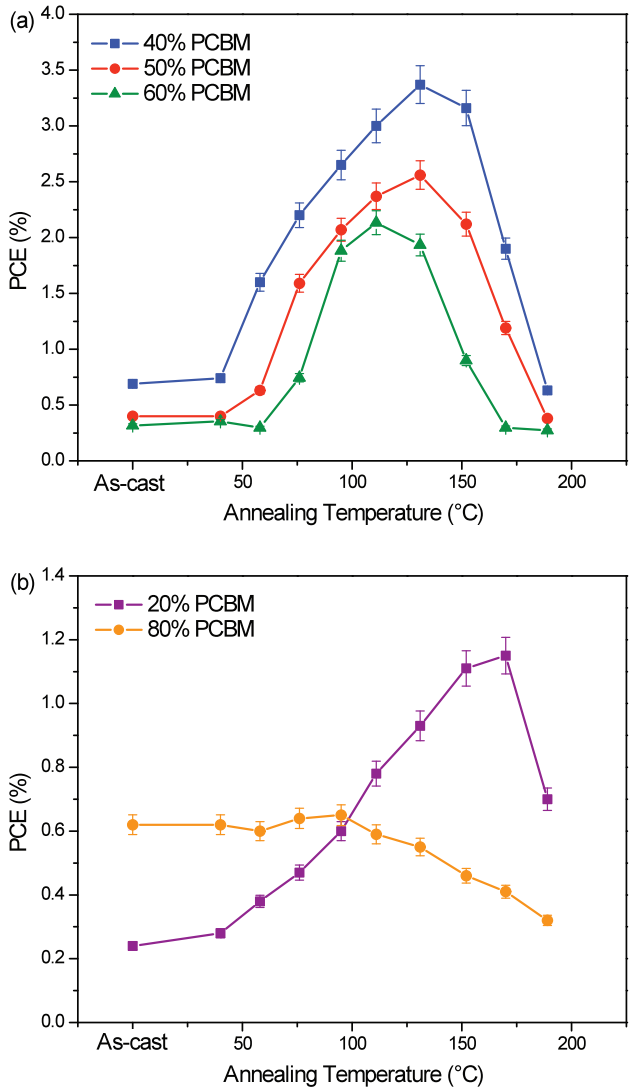

Figure 1. Power conversion efficiency (PCE) values for P3HT:PCBM blend devices as a function of annealing temperature. Data for devices having between 40 and 60 wt % PCBM in the active layer are shown in part a, while part b shows data for devices with 20 wt % and 80 wt % PCBM. Lines are provided as a guide only.

of 60:40 wt % P3HT:PCBM. The driving force for the improvements in device PCE come principally from changes in the short-circuit current density (J_{SC}), which can be seen from Figure S1, Supporting Information. We observe that the J_{sc} of each device blend composition qualitatively follows the same trend with annealing temperature as the PCE, increasing and then decreasing at temperatures that are apparently characteristic of the blend composition. We quantify this by defining T_{onset} as the temperature beyond which device efficiency is improved compared to an equivalent unannealed control. We find that T_{onset} increases from 45 ± 5 °C in devices with a film composition of 40 wt % PCBM, to 70 ± 5 °C in devices containing 60 wt % PCBM. At temperatures beyond T_{onset}, the PCE further increases, reaching an optimum value at a temperature we define as $T_{optimum}$. When annealed at a temperature above $T_{optimum}$ the PCE of devices is seen to decrease. We find that $T_{optimum}$ is also dependent on relative film composition, reducing from 130 ± 5 °C in a 40 wt % PCBM film to 110 ± 5 °C in film containing 60 wt % PCBM. Films

dx.doi.org/10.1021/ma202063k | Macromolecules 2012, 45, 1499–1508

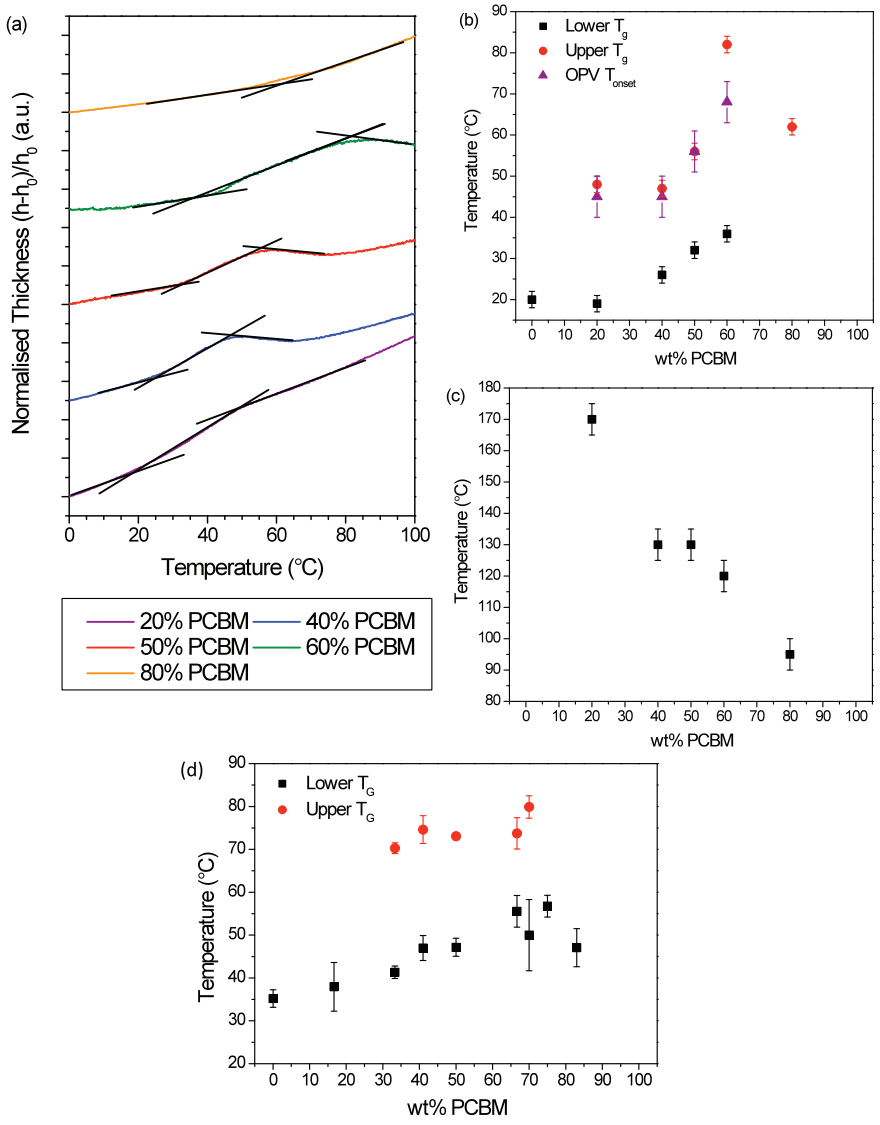

Figure 2. (a) Normalized thicknesses of P3HT:PCBM (wt %) thin films as a function of temperature during the first heating cycle. Data is offset for clarity. For each sample we fit a number of straight lines to the temperature-dependent expansion of the sample, with the intersection of such lines marking the apparent glass transitions of the blend. (b) Onset annealing temperature for PCE improvement in P3HT:PCBM OPVs as a function of the active layer composition, plotted alongside the T_g values extracted from part a. Optimum annealing temperatures for P3HT:PCBM OPVs as a function of the composition of the active layer composition are plotted in part c. T_g values for samples measured by DMTA are presented in part d.

containing a higher PCBM loading undergo a larger reduction in PCE when annealed at a temperature above $T_{optimum}$. For example, devices containing 40%, 50%, and 60% (wt %) PCBM within the active layer that have been annealed at 40 °C above $T_{optimum}$ have an efficiency that is 57, 47 and 42% of the efficiency of a device annealed at $T_{optimum}$.

In Figure 1b, we present a plot of the efficiency of devices having either a high or a low fraction of PCBM in its active layer. In both cases, we find that the PCE of the devices are low, with devices containing 20 wt % PCBM having a maximum efficiency of ~1.2%. The origin of such low efficiency is well understood,[22,23] as films composed predominantly of P3HT have favorable absorption characteristics, however exciton dissociation and extraction of electrons is inefficient due to an insufficient concentration of PCBM acceptor molecules. At high PCBM concentration however, the transport and extraction of holes becomes problematic together with a reduced absorption overlap of the active layer with the solar spectrum.[24]

For devices containing either 20% or 80 wt % PCBM, we see a change in device PCE on thermal annealing; for 20 wt % PCBM loading, we find values of T_{onset} and $T_{optimum}$ to be 50 ± 5 °C and 170 ± 5 °C respectively. When the device contains 80 wt % PCBM there is a negligible benefit from the thermal annealing process. Indeed, beyond approximately 105 °C the treatment becomes detrimental, with a monotonic decrease in PCE as the annealing temperature is increased.

From Figure S1, Supporting Information, it can also be seen that the fill-factor (*FF*) of the annealed devices is also improved by a factor of up to 2 times compared to that of the equivalent controls. We find that devices containing a high or a low fraction of PCBM undergo a smaller relative improvement compared to devices having a PCBM loading between 40 and 60 wt %. The relative magnitude of the *FF* provides an approximate measure of the relative balance between electron

dx.doi.org/10.1021/ma202063k | *Macromolecules* 2012, 45, 1499–1508

and hole mobilities,[9] with smaller *FF* indicating imbalanced charge-carrier mobility. Indeed, a number of studies have suggested that a *FF* less than ~42% indicates that charge-extraction is limited by space-charge.[25,26] The data in Figure S1 (Supporting Information) shows that for blend devices containing 20 wt % and 80 wt % PCBM, the *FF* never exceeds 37%, suggesting that such devices have highly imbalanced charge-carrier mobility.

To summarize; parts a and b of Figure 1 demonstrate that a clear composition-dependent annealing range exists. The onset temperature for improved device efficiency (T_{onset}) increases with increasing PCBM wt %, while the optimum annealing temperature ($T_{optimum}$) decreases with increasing PCBM wt %,. The effect of these two processes means that the annealing window for improving device PCE narrows with increasing PCBM wt %. Indeed, for devices containing the highest wt % of PCBM, thermal annealing is detrimental to device efficiency. We proceed to rationalize these findings on the basis of the various thermal transitions (including the apparent glass-transition temperature [T_g]) and properties of the active layer materials.

Our DMTA studies[18] indicate that when P3HT is blended with PCBM, the T_g of P3HT containing phases increase due to increased cohesive interactions between the P3HT and PCBM molecules. This observation indicates that the methanofullerene acts as an antiplastiser. Furthermore, our DMTA analysis demonstrated that this effect persists until the PCBM content becomes sufficiently high (66 wt %) whereupon the film undergoes phase-separation even within an unannealed film. This results in the formation of pure PCBM domains that lower the observed blend T_g, reflecting a reduced PCBM content in the mixed P3HT:PCBM phase.[18,27,28] Further analysis of this data shows that P3HT:PCBM blends with a PCBM composition between 33—75 wt % may actually have two T_gs, rather than a single T_g with a broad spread of values as implied previously. Either a relatively high or low T_g is observed in each sample by this technique, which we attribute to limitations in sensitivity or subtle variations in the drying time for the different samples. The general behavior of the system is shown in Figure 2d. As our spectroscopic ellipsometry data in Figure 2b show, both T_g are observed in films with 20—60 wt % PCBM, indicating that these transitions do occur in films that dry in an identical manner to OPV devices, and that therefore the two T_gs (as we will show) have an impact on the thermal annealing of OPV devices.

In the following work, we show these thermal measurements, coupled with spectroscopic ellipsometry, provide a useful framework in which to understand the effect of annealing on a P3HT:PCBM OPV device efficiency and hence be able to move away from empirically determinations of the optimum thermal treatments to apply. To do this, we have studied blend thin-films having thicknesses that are identical to those used in devices and have monitored their thermal expansion using spectroscopic ellipsometry during the first heating cycle. This method also permits us to quantify the various thermal transitions of the blend films, and permits us to reproduce the conclusions drawn from the DMTA. This is an important result, as it demonstrates that the results of our DMTA study also apply directly to device-applicable thin-films, whose thermal properties may differ from that of the bulk material.[29]

In Figure 2a, we plot the relative change in thickness of a series of blend thin-films as they are subjected to a thermal ramp. Specifically, we plot $(h - h_o)/h_o$ where h is the film thickness at temperature T and h_0 being the film thickness before thermal annealing. As shown, a number of changes occur in the thermal expansion rate as the films are annealed. We quantify the temperature at which these changes in expansion rate occur by fitting a straight line to the thermal expansion above and below each transition, a process that permits us to identify the temperature at which the transition occurs via the intersection of the fitted lines. We propose that these changes in slope occur at temperatures corresponding to the apparent glass transitions of the blends during the first heating cycle. In Figure 2b, we plot the T_g values extracted from part a, along with values for T_{onset} as determined from Figure 1, with $T_{optimum}$ values plotted in Figure 2c.

Using spectroscopic ellipsometry we have previously shown that thin-films of pure P3HT which is employed in this work have a T_g of 20 °C.[30] It can be seen in Figure 2a that in blends containing 20 wt % PCBM, there is a change in the thermal expansion rate that approximately coincides with this temperature with an additional higher temperature transition observed at 50 °C. For blend thin-films with 40−60 wt % PCBM, two transitions are again detectable, however the temperature of the T_g apparently increase as the relative content of PCBM within the blend is increased. At 80 wt % PCBM, a single transition is observed that occurs at a temperature that is relatively lower than that observed in the 60 wt % blend film. These results correlate well with the DMTA data shown in Figure 2d, again suggesting the occurrence of two T_g's across the midcomposition range.

In many cases, we find that as a film is heated above the thermal-transitions, the expansion rate remains positive. We assert that these transitions correspond to glass-transitions, with an expansion in film thickness occurring as the molecules acquire sufficient thermal energy to undergo a transition to a more mobile state and thus explore a greater free volume. A notable exception to this occurs in blends with a PCBM loading of 40−60 wt % in which the films undergo an apparent contraction in thickness when heated above the second T_g. We have previously shown in a P3HT:PCBM blend (40 wt % PCBM) that the glass transition is convoluted with the effects of the removal of residual casting solvent during first heating cycle.[30] Note that this transition is determined by the thermal properties of the blend and not the casting solvent. We are confident in this assertion as the temperature at which this process occurs is far below the boiling point of the chlorobenzene solvent used to cast the films (132 °C). It appears therefore that as the film is heated above the high temperature T_g, solvent loss occurs as the polymer chains have sufficient thermal energy to allow the expulsion of trapped solvent molecules. This loss of solvent will clearly lead to a partial self-organization of the polymer that will manifest itself by a reduction in film thickness. This volume-reduction process will dominate the competing process of thermal expansion until such a time where the majority of the solvent has been removed. At this stage the expansion rate of the sample becomes positive once more. We have estimated the volume fraction of trapped solvent by extrapolating the thermal expansion of blend thin-films below T_g to the point where the majority of solvent is presumed to have left the sample. This is defined as the local minima in the thickness-temperature data presented in Figure 2a. We estimate the volume fraction of solvent trapped in the as-cast films as 1.3%, 1.8%, and 3.2% for blends with 40, 50 and 60 wt % PCBM respectively. The increase in trapped solvent with increasing PCBM wt % is

consistent with the relatively higher T_g of these films (a blend with a higher T_g is likely to trap more solvent).

It can be seen that this solvent-loss process is not observed in blend films containing either 20 wt % or 80 wt % of PCBM. We believe that this phenomena has two different origins. First the absence of solvent loss effects in blend films containing 80 wt % PCBM blend reflects the fact the relatively low concentration of P3HT molecules within the film limits its ability to trap solvent. Second, it has been shown that as temperature difference between the temperature at which a film is cast and the T_g of film increases, a larger volume of the casting solvent is trapped.[30] As the T_g of films containing 20 wt % PCBM lies below room temperature, it suggests that the majority of casting solvent evaporates as the film is cast and thus little solvent remains to be expelled as the film is annealed.

As can be seen in Figure 2b, the T_g of P3HT:PCBM blend thin-films is larger than the T_g of the pure polymer. Furthermore this temperature increases as the relative wt % of PCBM in the blend is increased. This result is in good agreement with our previous study of this system using DMTA. It can also be seen that in the blend thin-film having the highest loading of PCBM (80 wt %), the T_g of the blend undergoes a reduction; an observation also in line with our earlier findings. The measurements presented here however indicate that in blends composed of between 20 and 60 wt % PCBM, there are in fact two distinct glass transitions. As far as we are aware, this is the first observation of such a phenomena for this system; a result we interpret in terms of the blend film comprising at least two compositionally distinct amorphous P3HT-rich phases within the blend thin-film. We emphasize that these phases coexist with the pure crystalline P3HT and PCBM phases. For many mixtures of polymers with small molecules, such phase separation is not uncommon, because of the limited solubility of the polymer in the crystalline small molecule phase.[31] However, there may be other possible explanations which will be touched on below.

To gain confidence in the existence of a phase associated with the low temperature T_g, we have measured the thermal expansion of a 50 wt % PCBM blend thin-film over the course of two heating and cooling cycles. This data is presented in Figure 3, where parts a and b correspond to the first heating and cooling respectively of the film when raised to a temperature of 50 °C. Parts c and d similarly correspond to the second heating and cooling of the same film when raised to 100 °C. We have also used SE to determine the wavelength-dependent extinction coefficient of the film as shown in part e. As can be seen in parts a–c of Figure 3, the transition around 35 °C is measurable during heating, which shifts to 25 °C as the sample is cooled. The apparent reversibility of this transition (recorded at 30 °C during the second heating cycle) within the range of heating temperatures applied suggests its origin is a glass transition within the blend. Upon cooling from a temperature above the second higher temperature T_g (see Figure 3d), we find that only a single transition at 50 °C can be detected. In Figure 3e, it can be seen that the extinction coefficient of the film remains relatively unchanged after the first heating and cooling cycle, but undergoes a significant enhancement in oscillator-strength that is accompanied by a red-shift after the second heating and cooling cycle. This suggests that heating the film above the low temperature T_g does not induce significant morphological changes within the film; an observation that we believe suggests that the phase

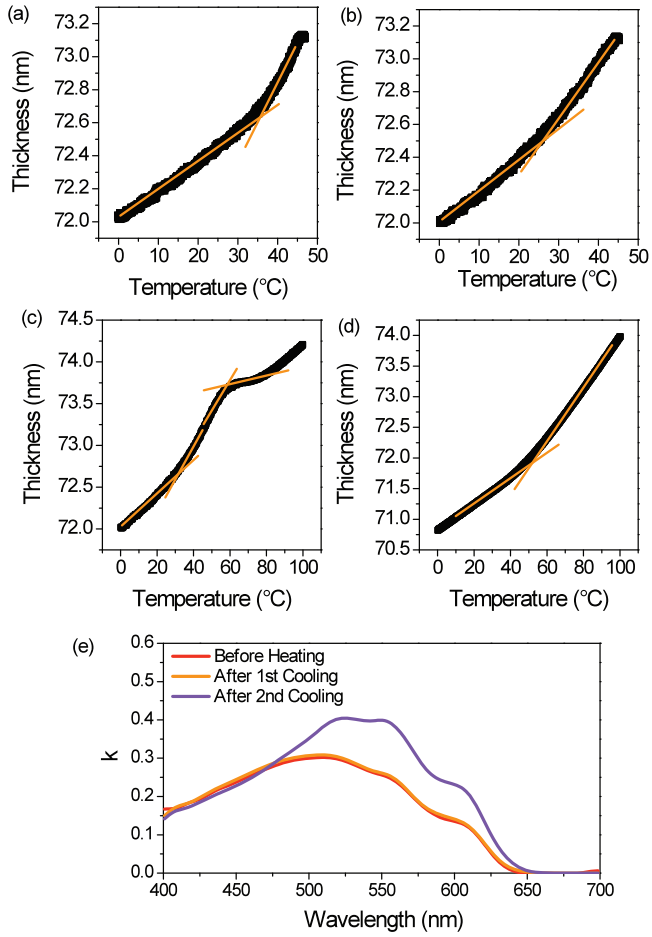

Figure 3. Thickness changes for a P3HT:PCBM (50:50 wt %) blend thin film during (a) first heating, (b) first cooling, (c) second heating, and (d) second cooling. Heating and cooling rate was kept at 5 °C/min throughout. The intersections of the orange lines mark the apparent T_g (s) of the sample. In part e, the modeled extinction coefficient spectrum for the blend before heating and after the first and second heating cycles.

associated with this transition comprises a relatively low volume-fraction of the film.

In Figure 2b, we plot the T_g values extracted from the SE data as a function of PCBM wt % in the blend, alongside the onset temperature for OPV device improvement, as determined from the data in Figure 1. Notably, a close coincidence is found between T_{onset} (for the OPVs) and the upper temperature T_g of the blends. This agreement confirms the T_g of the blend defines the minimum effective temperature for improving the photocurrent generating efficiency of the blend and, in the most efficient blend compositions, for the removal of residual solvent. The positive correlation between device data and T_g data suggests that at these annealing temperatures the major driving force for device improvement are morphological changes which occur in the bulk of the blend film, with interfacial effects playing an apparently relatively minor role.

It is important to acknowledge the differences between the samples prepared for SE and for OPVs. We have endeavored to replicate in the samples for SE as closely as possible the morphology of P3HT:PCBM blends as would exist in an OPV prior to annealing. However, for SE samples a free surface exists which is not present during the annealing process for OPVs. Additionally the films are cast onto native silicon oxide and not

dx.doi.org/10.1021/ma202063k | Macromolecules 2012, 45, 1499–1508

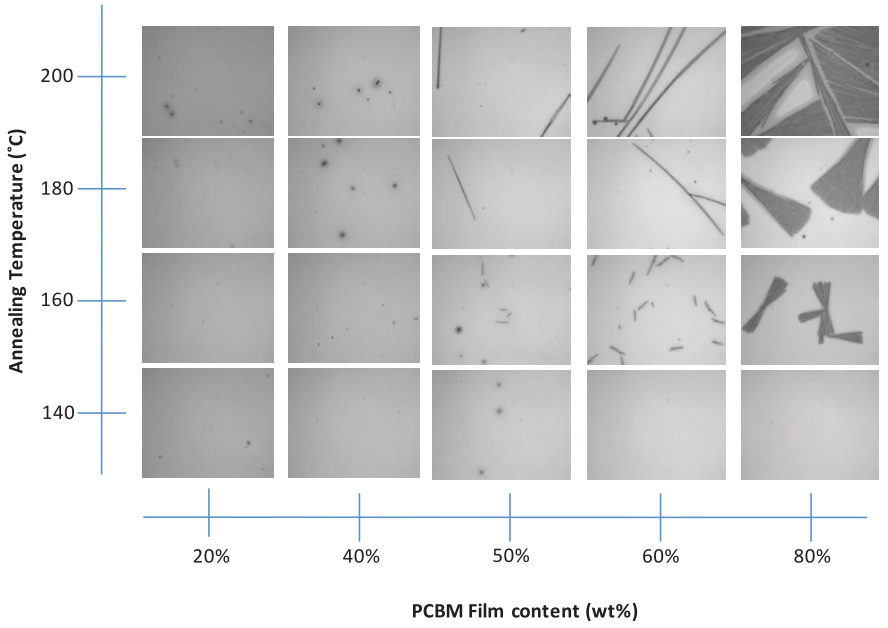

Figure 4. Optical micrographs (60 μm × 80 μm field of view) for P3HT:PCBM blend thin-films annealed and subsequently cooled from a temperature above 140 °C.

PEDOT:PSS. It is not possible to model both thickness changes and optical characteristics of films beneath 100 nm of aluminum, which would fully resemble a device and so would be the ideal sample. We have monitored a blend thin film cast onto PEDOT:PSS during heating, in addition to a control sample of PEDOT:PSS only. The modeled thicknesses, presented in the Supporting Information, Figure S3, shows that PEDOT:PSS undergoes a thickness contraction in the low temperature range up to 70 °C. For blend thin-films cast onto PEDOT:PSS this transition overlaps with the low T_g transitions identified for samples on native silicon oxide. However, it is problematic to deconvolute these two processes. A number of studies[32−34] have identified a P3HT rich surface layer in as-cast blend thin-films on PEDOT:PSS or native silicon oxide. This surface driven phase separation may be the origin of the low T_g seen in the SE sample, but at this stage this identification cannot be verified. Furthermore, the absolute volume fraction of this layer will differ depending upon the substrate used and the consequent balance of surface and interfacial energy terms, so that quantification of the volume fraction would be nontrivial. However, since the DMTA samples are much thicker, it is possible this explains why the sensitivity to detect a thin surface layer is too small reliably to see the appearance of two T_g's in a single DMTA sample.

We also note that the thin-films studied here may exhibit characteristics of optical anisotropy,[34] a consequence of the ability of P3HT chains to partially crystallize edge-on with respect to the sample substrate. However, as stated in the Experimental Section, film thicknesses are modeled in wavelength range in which the film is transparent (700−1000 nm). In this range, the absorption is close to zero, and the refractive index changes due to anisotropy are marginal. We do not expect the optical anisotropy to significantly affect the SE measurement as the phase behavior can also be determined from the raw ellipsometric data[29] (specifically Ψ, the amplitude ratio of the reflected and incident light beams). An example of identifying phase transitions using Ψ vs temperature is shown in the Supporting Information, Figure S4

We now focus our attention on the effect of annealing a blend above its T_g. With the exception of the devices based on a blend containing 80 wt % PCBM, thermal annealing at temperatures up $T_{optimum}$ increases device efficiency by driving phase separation and increasing the crystallinity of each phase.[35] Beyond $T_{optimum}$ it is possible for at least one of the materials within the film to undergo excessive phase separation or a phase-transition, resulting in a morphology that is less favorable for efficient device operation. In Figure 2c, we plot the optimum annealing temperature as a function of PCBM wt %. It can be seen that this temperature undergoes a progressive reduction as the fraction of PCBM is increased. As we discuss later, this temperature is most likely defined by the kinetics of the annealing process, rather than being associated with any one thermal transition. We note however that pure PCBM undergoes cold crystallization at around 155 °C using DMTA.[18] GIWAXS has been used to measure this transition at 148 °C for pure PCBM, with a shift to lower temperatures in P3HT:PCBM blends.[36]

To explore the apparent observation of an optimum annealing temperature, we have performed optical microscopy on a series of P3HT:PCBM blend films having a range of different relative compositions that were annealed at a series of temperatures above 140 °C and subsequently cooled rapidly to room temperature. A selection of representative images is shown in Figure 4. As can be seen, after thermal annealing at 140 °C, (a temperature that just exceeds $T_{optimum}$ for all devices with the exception of the 20:80 wt % P3HT:PCBM active layer blend) few structures are present that can be resolved optically in all of the films studied. These observations suggest that films annealed below this temperature mainly consist of nanoscale domains of P3HT and PCBM together with a molecularly mixed phase. However as the annealing temperature is raised above 140 °C, it can be seen that excessive phase separation between the blend components occurs. Indeed, aggregates having a size of 10 to 100 s of micrometers, that we identify as polycrystalline PCBM,[36] form in films composed of 80 wt % PCBM that have been annealed at a temperature above 140 °C,

dx.doi.org/10.1021/ma202063k | *Macromolecules* 2012, 45, 1499−1508

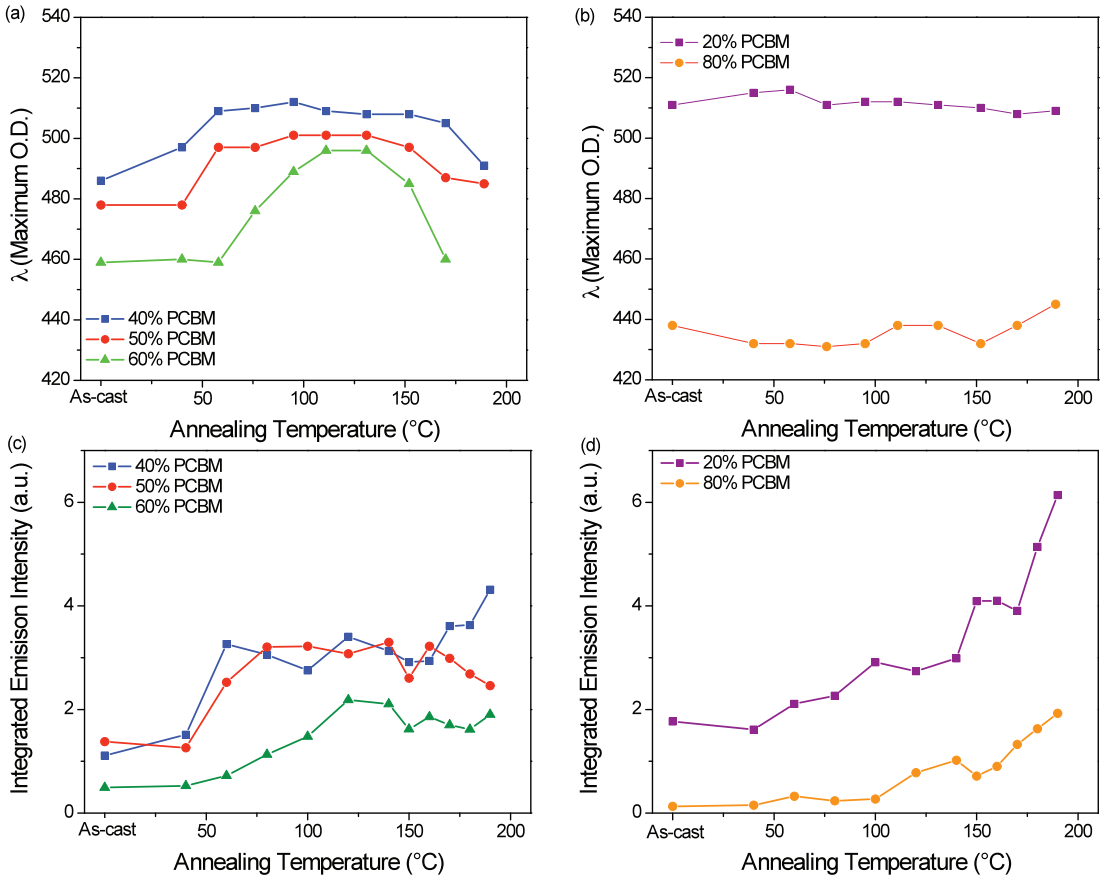

Figure 5. The wavelength at which blend thin-film optical density is maximized, λ_{max}, after thermal annealing for (a) blends with 40−60 wt % PCBM and (b) 20 wt % and 80 wt % PCBM. (c and d) Integrated photoluminescence emission from samples after annealing for blends with 40−60 wt % PCBM and 20 wt % or 80 wt % PCBM respectively. Lines are provided as a guide only.

in agreement with the PCBM solid−solid transition which we measure at 155 °C. As the relative fraction of PCBM is reduced, fewer microscopic PCBM crystallites are observed at any given annealing temperature, reflecting the fact that a smaller number of PCBM molecules are present in the sample. We believe that this observation provides a partial explanation for the relative stability of devices having a low PCBM fraction when annealed at a temperature just above $T_{optimum}$ as discussed earlier, since excessive phase separation is clearly hindered by the relatively low concentration of PCBM.

We note that the precise onset of excessive phase separation will be highly sensitive to the annealing time and exact conditions of sample preparation, including the casting solvent and the properties of the polymer (for example its molecular weight and regioregularity). However, the correlation between excessive (micrometer-scale) phase separation and the reduction in the optimum annealing temperature for devices with increasing wt % PCBM has important consequences for future polymer:PCBM blend OPVs where the optimum blend composition has not been determined. If thermal annealing is employed as a potential route for improving device efficiency with differing polymer:fullerene combinations, a range of temperatures should be employed to account for the possibility that PCBM molecules aggregate excessively when present in large weight fractions within the blend thin-film.

The existence of microscopic PCBM aggregates in P3HT:PCBM blend films is a clear indication that the film has been overannealed, resulting in reduced operational efficiency. We note that such structures may also be sufficiently large to exceed film thickness, thereby creating a short-circuit or damaging the device electrode.[37] The formation of such microscopic structures by annealing above $T_{optimum}$ will be accompanied by a relative depletion of acceptor material within the bulk of the film; an effect that will reduce both the efficiency of exciton dissociation and the extraction of electrons from the device. Nevertheless, we find that the optimum annealing temperature for OPVs occurs before the onset on PCBM micrometer-scale aggregation. To further characterize the effects of annealing on the properties of P3HT:PCBM based devices, we have measured both the optical density and relative photoluminescence efficiency of a series of representative films. Such measurements provide a useful probe to qualitatively explore structure−property relationships of the blend films at a length-scale (up to ∼10 nm) that cannot be accessed using conventional optical microscopy techniques, thereby providing a suitable compliment to the earlier discussion.

In Figure 5, we present a summary of the optical characteristics of the blend thin-films as a function of the annealing temperature. For ease of comparison, the data is split in the same manner as in Figure 1. Specifically, parts a and b of Figure 5 show the wavelength at which blend thin-films have their peak optical density (here defined as λ_{max}), while parts c and d show the integrated photoluminescence emission intensity of the same films. We also present representative spectra from which this data is extracted in the Supporting Information (Figures S5 and S6).

dx.doi.org/10.1021/ma202063k | *Macromolecules* 2012, 45, 1499−1508

It can be seen that annealing films containing between 40 and 60 wt % PCBM at a relatively low temperature results in a red-shift of λ_{max}. For example, a film containing 40 wt % PCBM undergoes a shift in λ_{max} from 485 nm to 515 nm after being annealed at 130 °C. In Figure S5, Supporting Information, it can be seen that this red-shift is also accompanied by an increase in optical density. We find this trend reverses (i.e., the optical density decreases and λ_{max} undergoes a relative blue-shift) after a film is annealed beyond a temperature approximately coincident with $T_{optimum}$. In fact, a clear correlation is found between the data in Figures 1a and 4a, showing that the increased device PCE on annealing above T_{onset} (T_g) is correlated with a red-shift of λ_{max} and an increase in OD, while annealing above $T_{optimum}$ is correlated with a blue-shift of λ_{max} and a reduction in OD. This demonstrates that annealing a P3HT:PCBM film at a temperature between T_{onset} and $T_{optimum}$, followed by cooling to room-temperature provides a driving force for P3HT crystallization, providing a partial explanation for improvements in device efficiency (for example, improved harvesting of the solar spectrum). On annealing a film above $T_{optimum}$, followed by a relatively rapid return to room temperature, the observed blue-shift of λ_{max} and relative weakening in film OD suggests that a significant fraction of the P3HT polymer is quenched into a largely amorphous state. Note that this process occurs without the film being partially melted, as the melt temperature of P3HT is expected to be above 200 °C for all the blend compositions explored in this work.[18,20] Nevertheless, this rapid return to room-temperature generates a film having poor light harvesting capability and lowered charge mobility.[38] Note however that we have previously shown that by slowly cooling blend thin-films even from relatively high (>150 °C) temperatures, polymer crystallization can be encouraged.[30]

It is apparent that the maximum OD of a film on annealing is inversely correlated with the relative PCBM concentration. As the maximum absorption wavelength λ_{max} is a measure of the degree of crystallization, this effect shows that an increased PCBM concentration hinders P3HT crystallization. Interestingly, Figure 5b demonstrates that films containing either a high or low PCBM weight fraction only undergo small changes in λ_{max} on annealing. On closer inspection of absorption spectra recorded from films containing a relatively low (20 wt %) concentration of PCBM (see Supporting Information, Figure S4a), it can be seen that even in as-cast films, there is a relative high fraction of crystalline P3HT present (as evidenced by the 0−0 vibronic peak seen around 600 nm) that is not significantly increased by subsequent thermal annealing. In films containing a high fraction (80 wt %) of PCBM, the packing and partial crystallization of P3HT is clearly restricted by the PCBM under the annealing protocol used in this work.

In parts a and b in Figure 5, we plot the integrated PL intensity from a series of thin-film blends as a function of annealing temperature. We find that the relative PL intensity is inversely proportional to the fraction of PCBM as anticipated. It can be seen that for each of the film compositions, the PL emission intensity increases once the annealing temperature exceeds a certain threshold temperature, again closely correlated to T_g and T_{onset}. The effect is particularly evident in films containing either 40 or 50 wt % PCBM, where PL emission intensity increases significantly on annealing above 50 °C, while emission from films containing 60 wt % PCBM increases in a linear fashion when annealed above 60 °C. The temperature at which the PL emission intensity increases also correlates well with observed changes in the absorption spectra (Figure 5, parts a and b) and device efficiency (Figure 1, parts a and b). Such correlated trends further suggest that annealing above T_{onset} permits the film morphology to undergo a transition from a largely mixed phase in which excitons are efficiently quenched, to a morphology in which nanoscale phase separation reduces the efficiency of exciton dissociation.

When thin films containing a relatively low fraction of PCBM are annealed at temperatures above 150 °C, we observe a marked increase in PL intensity. This increase in PL intensity is indicative of reduced exciton quenching resulting from the formation of larger (or purer) P3HT domains. In contrast, the fluorescence intensity from films containing 50 wt % by mass PCBM does not increase significantly on being annealed above 150 °C. Our measurements of the absorption spectra indicate that P3HT has limited ability to undergo self-organization in films containing a relatively high fraction of PCBM and thus such films are likely to contain a greater (relative) fraction of amorphous P3HT. We speculate therefore that the relatively small increases in P3HT PL emission intensity from films containing a relatively high fraction of PCBM on annealing results from PCBM molecules that have become mixed in regions dominated by amorphous polymer.[27,28] Such amorphous material may hinder the ability of PCBM to coalesce to form nanoscale networks upon thermal annealing, with such molecular-mixed phases being associated with relatively efficient exciton quenching.

In summary, the data presented in Figures 4 and 5 demonstrate that annealing a P3HT:PCBM film beyond $T_{optimum}$ results in both P3HT and PCBM blend fractions that have unfavorable OPV characteristics. This may arise from reduced optical density and overlap with the solar spectrum (limiting the ability of the device to harvest sunlight), as shown in Figure 4, and from the creation of microscopic PCBM aggregates, reducing its ability to disassociate excitons and transport charges as shown in Figure 3. Although we have been unable to ascribe a thermal transition to $T_{optimum}$, as we have demonstrated when correlating T_{onset} with the higher-temperature T_g of P3HT, it is likely that $T_{optimum}$ is instead determined by the kinetics of PCBM diffusion during isothermal annealing and the relative crystallinity of both P3HT and PCBM during annealing and cooling. Thus the upper bound of beneficial annealing temperatures will be sensitive to the exact conditions of sample preparation. Nevertheless, the observed trend that a relatively higher wt % of PCBM within an OPV lowers the optimum temperature range due to its propensity for excessive phase separation is likely to be general in polymer-fullerene blends and should be taken into account when exploring systems where the optimum film composition is unknown.

■ CONCLUSIONS

We have explored the impact of thermal annealing on the photovoltaic efficiency of P3HT:PCBM OPVs across a range of active layer compositions and annealing temperatures. These results are related to the phase transition behavior of the blends. Our measurements on the glass transition of the blend thin-films suggest that two distinct compositional amorphous phases exist. We demonstrate a positive correlation between the highest temperature apparent glass transition and the minimum temperature necessary to improve the efficiency of an OPV device. This confirms that annealing a film above its glass transition temperature (for that particular blend composition) will permit molecules to undergo cooperative motion, forming

a morphology that can promote efficient photocurrent generation.

We have also identified a blend-ratio dependent optimum annealing temperature for efficient device operation. This has been rationalized in terms of excessive phase separation by PCBM, and the reduced ability of the blend thin-film to harvest sunlight. As the wt % of PCBM within the blend increases, the optimum temperature decreases, from 170 °C to as low as 100 °C. We have also found that thermally annealing devices that contain a high weight fraction of PCBM apparently results in a reduction in operational efficiency only; a result that may be particularly relevant in OPVs based on amorphous low energy band gap polymers in which large relative fractions of fullerenes are often used.[39,40]

Our results demonstrate therefore that the optimum annealing temperature of an OPV device based on a polymer/fullerene blend is a function of the relative composition of the blend; an effect that we have related to the phase transition properties of the film and in particular its glass transition temperature. This is an important observation, as it indicates that phase transition characterization of unexplored polymer−fullerene systems should be performed in parallel with device optimization studies, with the glass-transition temperature of each particular polymer−fullerene blend film providing a strong indication of the minimum annealing temperature beyond which changes in device efficiency can be anticipated.

EXPERIMENTAL SECTION

Samples were prepared using P3HT (Rieke, 4002-E), PCBM (Solenne, 99% purity) and chlorobenzene (Aldrich, anhydrous, 98% purity). All materials were used as received and were not subject to additional purification protocols. All samples were prepared within an overpressure dry nitrogen glovebox. To fabricate blend solutions, P3HT and PCBM were first dissolved separately at 25 mg/mL into chlorobenzene. These solutions were then heated at 70 °C until all material was fully dissolved and then rapidly cooled to room temperature (to minimize the effects of gelation[41]), after which they were passed through a 0.45 μm PTFE filter before being blended by volume to the required composition.

OPV devices were fabricated following a method described in detail elsewhere.[42] In this work, P3HT:PCBM solutions were spin-cast forming films having a thickness of 70 ± 4 nm as measured by profilometry (Dektak 150). In all cases, spin-speed was adjusted to compensate for variations in blend solution viscosity. A series of identical control films were also prepared for spectroscopic measurements. OPV devices were subjected to thermal annealing after the vacuum deposition of a 100 nm thick aluminum cathode. This thermal anneal step was performed by placing the device substrate onto a hot plate for 10 min after which they were transferred onto a copper plate held at room temperature, facilitating rapid cooling. The PCE of encapsulated devices were determined using a Newport Solar Simulator (25 °C at 100 mW cm^{-2}) having an NREL calibrated output.

DMTA samples were drop-cast from 50 mg/mL solutions that were preheated to 70 °C onto stainless steel material pockets that were folded to enclose the film, as described previously.[18] This was performed under flowing nitrogen. Spectroscopic ellipsometry was performed on representative films cast on a silicon substrate using a M2000v, J. A. Woollam Co., ellipsometer. For measurement, films were placed on an adapted Linkam stage and heated at a rate of 5 °C/minute up to 250 °C. All measurements were performed under nitrogen. To determine film thickness from ellipsometry, a Cauchy model was applied over the spectral region where the samples were optically transparent (700−1000 nm).[43] Modeled thicknesses provided a boundary condition for the calculation of the film extinction coefficient using a b-spline model.[43] The thermal expansion of the samples during heating was used to extract the T_g using methods described elsewhere.[29] UV−vis absorption and photoluminescence (PL) of thin films were measured using a Horiba Fluoromax spectrometer. PL spectra were acquired following excitation at 500 nm and were corrected for thin-film absorption effects. Integrated PL emission values were calculated over a wavelength range of 600−800 nm.

ASSOCIATED CONTENT

Supporting Information

Device metrics for all devices fabricated (Figure S1) and characteristics of optimized devices (Figure S2). Additional ellipsometry data (Figures S3 and S4) and representative OD and PL spectra of P3HT:PCBM blend thin-films (Figures S5 and S6 respectively). This material is available free of charge via the Internet at http://pubs.acs.org.

AUTHOR INFORMATION

Corresponding Author

*E-mail: (A.J.P.) a.j.pearson@sheffield.ac.uk; (D.G.L.) d.g.lidzey@sheffield.ac.uk.

ACKNOWLEDGMENTS

We thank EPSRC for financial support via the grant "Optimization of polymer photovoltaic devices through control of phase separation" (Grant references EP/F016433/1 and EP/F019297/1). A.J.P. acknowledges an award of an EPSRC DTA Ph.D. studentship.

REFERENCES

(1) Brabec, C. J.; Gowrisanker, S.; Halls, J. J. M.; Laird, D.; Jia, S. J.; Williams, S. P. *Adv. Mater.* **2010**, *22* (34), 3839−3856.
(2) Krebs, F. C. *Sol. Energy Mater. Sol. Cells* **2009**, *93* (4), 465−475.
(3) Krebs, F. C. *Sol. Energy Mater. Sol. Cells* **2009**, *93* (4), 394−412.
(4) Boudreault, P. L. T.; Beaupre, S.; Leclerc, M. *Polym. Chem.* **2010**, *1* (2), 127−136.
(5) Allard, N.; Aich, R. B.; Gendron, D.; Boudreault, P. L. T.; Tessier, C.; Alem, S.; Tse, S. C.; Tao, Y.; Leclerc, M. *Macromolecules* **2010**, *43* (5), 2328−2333.
(6) Helgesen, M.; Sondergaard, R.; Krebs, F. C. *J. Mater. Chem.* **2010**, *20* (1), 36−60.
(7) Liang, Y. Y.; Xu, Z.; Xia, J. B.; Tsai, S. T.; Wu, Y.; Li, G.; Ray, C.; Yu, L. P. *Adv. Mater.* **2010**, *22* (20), E135−+.
(8) Ma, W. L.; Yang, C. Y.; Gong, X.; Lee, K.; Heeger, A. J. *Adv. Funct. Mater.* **2005**, *15* (10), 1617−1622.
(9) Li, G.; Shrotriya, V.; Huang, J. S.; Yao, Y.; Moriarty, T.; Emery, K.; Yang, Y. *Nat. Mater.* **2005**, *4* (11), 864−868.
(10) Li, G.; Yao, Y.; Yang, H.; Shrotriya, V.; Yang, G.; Yang, Y. *Adv. Funct. Mater.* **2007**, *17* (10), 1636−1644.
(11) Campoy-Quiles, M.; Ferenczi, T.; Agostinelli, T.; Etchegoin, P. G.; Kim, Y.; Anthopoulos, T. D.; Stavrinou, P. N.; Bradley, D. D. C.; Nelson, J. *Nat. Mater.* **2008**, *7* (2), 158−164.
(12) Clarke, T. M.; Ballantyne, A. M.; Nelson, J.; Bradley, D. D. C.; Durrant, J. R. *Adv. Funct. Mater.* **2008**, *18* (24), 4029−4035.
(13) Beal, R. M.; Stavrinadis, A.; Warner, J. H.; Smith, J. M.; Assender, H. E.; Watt, A. A. R. *Macromolecules* **2010**, *43* (5), 2343−2348.
(14) Yang, X.; Loos, J. *Macromolecules* **2007**, *40* (5), 1353−1362.
(15) Blom, P. W. M.; Mihailetchi, V. D.; Koster, L. J. A.; Markov, D. E. *Adv. Mater.* **2007**, *19* (12), 1551−1566.
(16) Li, G.; Shrotriya, V.; Yao, Y.; Yang, Y. *J. Appl. Phys.* 2005, *98*, (4), -.
(17) Kim, Y.; Cook, S.; Tuladhar, S. M.; Choulis, S. A.; Nelson, J.; Durrant, J. R.; Bradley, D. D. C.; Giles, M.; McCulloch, I.; Ha, C. S.; Ree, M. *Nat. Mater.* **2006**, *5* (3), 197−203.

(18) Hopkinson, P. E.; Staniec, P. A.; Pearson, A. J.; Dunbar, A. D. F.; Wang, T.; Ryan, A. J.; Jones, R. A. L.; Lidzey, D. G.; Donald, A. M. *Macromolecules* **2011**, *44* (8), 2908−2917.
(19) Zhao, J.; Swinnen, A.; Van Assche, G.; Manca, J.; Vanderzande, D.; Van Mele, B. *J. Phys. Chem. B* **2009**, *113* (6), 1587−1591.
(20) Muller, C.; Ferenczi, T. A. M.; Campoy-Quiles, M.; Frost, J. M.; Bradley, D. D. C.; Smith, P.; Stingelin-Stutzmann, N.; Nelson, J. *Adv. Mater.* **2008**, *20* (18), 3510−+.
(21) Padinger, F.; Rittberger, R. S.; Sariciftci, N. S. *Adv. Funct. Mater.* **2003**, *13* (1), 85−88.
(22) Baek, W. H.; Yoon, T. S.; Lee, H. H.; Kim, Y. S. *Org. Electron.* **2010**, *11* (5), 933−937.
(23) van Bavel, S. S.; Barenklau, M.; de With, G.; Hoppe, H.; Loos, J. *Adv. Funct. Mater.* **2010**, *20* (9), 1458−1463.
(24) Wienk, M. M.; Kroon, J. M.; Verhees, W. J. H.; Knol, J.; Hummelen, J. C.; van Hal, P. A.; Janssen, R. A. J. *Angew. Chem., Int. Ed.* **2003**, *42* (29), 3371−3375.
(25) Mihailetchi, V. D.; Wildeman, J.; Blom, P. W. M. *Phys. Rev. Lett.* **2005**, *94*, 12.
(26) Goodman, A. M.; Rose, A. *J. Appl. Phys.* **1971**, *42* (7), 2823−&.
(27) Treat, N. D.; Brady, M. A.; Smith, G.; Toney, M. F.; Kramer, E. J.; Hawker, C. J.; Chabinyc, M. L. *Adv. Energy Mater.* **2011**, *1* (1), 82−89.
(28) Collins, B. A.; Gann, E.; Guignard, L.; He, X.; McNeill, C. R.; Ade, H. *J. Phys. Chem. Lett.* **2010**, *1* (21), 3160−3166.
(29) Keddie, J. L.; Jones, R. A. L.; Cory, R. A. *Europhys. Lett.* **1994**, *27* (1), 59−64.
(30) Wang, T.; Pearson, A. J.; Lidzey, D. G.; Jones, R. A. L. *Adv. Funct. Mater.* **2011**, *21* (8), 1383−1390.
(31) Jones, R. A. L.; Richards, R. W., *Polymers at surfaces and interfaces*. Cambridge University Press: Cambridge, U.K., 1999.
(32) Parnell, A. J.; Dunbar, A. D.; Pearson, A. J.; Staniec, P. A.; Dennison, A. J.; Hamamatsu, H.; Skoda, M. W.; Lidzey, D. G.; Jones, R. A. *Adv. Mater.* **2010**, *22* (22), 2444−7.
(33) Tillack, A. F.; Noone, K. M.; MacLeod, B. A.; Nordlund, D.; Nagle, K. P.; Bradley, J. A.; Hau, S. K.; Yip, H.-L.; Jen, A. K. Y.; Seidler, G. T.; Ginger, D. S. *ACS Appl. Mater. Interfaces* **2011**, *3* (3), 726−732.
(34) Germack, D. S.; Chan, C. K.; Kline, R. J.; Fischer, D. A.; Gundlach, D. J.; Toney, M. F.; Richter, L. J.; DeLongchamp, D. M. *Macromolecules* **2010**, *43* (8), 3828−3836.
(35) Nguyen, L. H.; Hoppe, H.; Erb, T.; Gunes, S.; Gobsch, G.; Sariciftci, N. S. *Adv. Funct. Mater.* **2007**, *17* (7), 1071−1078.
(36) Verploegen, E.; Mondal, R.; Bettinger, C. J.; Sok, S.; Toney, M. F.; Bao, Z. A. *Adv. Funct. Mater.* **2010**, *20* (20), 3519−3529.
(37) Chirvase, D.; Parisi, J.; Hummelen, J. C.; Dyakonov, V. *Nanotechnology* **2004**, *15* (9), 1317−1323.
(38) Erb, T.; Zhokhavets, U.; Gobsch, G.; Raleva, S.; Stuhn, B.; Schilinsky, P.; Waldauf, C.; Brabec, C. J. *Adv. Funct. Mater.* **2005**, *15* (7), 1193−1196.
(39) Blouin, N.; Michaud, A.; Gendron, D.; Wakim, S.; Blair, E.; Neagu-Plesu, R.; Belletete, M.; Durocher, G.; Tao, Y.; Leclerc, M. *J. Am. Chem. Soc.* **2008**, *130* (2), 732−742.
(40) Beiley, Z. M.; Hoke, E. T.; Noriega, R.; Dacuna, J.; Burkhard, G. F.; Bartelt, J. A.; Salleo, A.; Toney, M. F.; McGehee, M. D. *Adv. Energy Mater.* **2011**, *1* (5), 954−962.
(41) Koppe, M.; Brabec, C. J.; Heiml, S.; Schausberger, A.; Duffy, W.; Heeney, M.; McCulloch, I. *Macromolecules* **2009**, *42* (13), 4661−4666.
(42) Kingsley, J. W.; Green, A.; Lidzey, D. G. *Proc. SPIE—Int. Soc. Opt. Eng.* **2009**, *7416*, 74160T.
(43) Wang, T.; Dunbar, A. D. F.; Staniec, P. A.; Pearson, A. J.; Hopkinson, P. E.; MacDonald, J. E.; Lilliu, S.; Pizzey, C.; Terrill, N. J.; Donald, A. M.; Ryan, A. J.; Jones, R. A. L.; Lidzey, D. G. *Soft Matter* **2010**, *6* (17), 4128−4134.